

Article

Not peer-reviewed version

In Vitro Hemostatic Activity of Novel Fish Gelatin- Alginate Sponge (FGAS) Prototype

[Heri Herliana](#)*, [Harmas Yazid Yusuf](#), [Avi Laviana](#), [Ganesha Wandawa](#), Basril Abbas

Posted Date: 14 May 2024

doi: 10.20944/preprints202405.0934.v1

Keywords: Fish gelatin; alginate; hemostatic sponge; blood coagulation



Preprints.org is a free multidiscipline platform providing preprint service that is dedicated to making early versions of research outputs permanently available and citable. Preprints posted at Preprints.org appear in Web of Science, Crossref, Google Scholar, Scilit, Europe PMC.

Copyright: This is an open access article distributed under the Creative Commons Attribution License which permits unrestricted use, distribution, and reproduction in any medium, provided the original work is properly cited.

Article

In Vitro Hemostatic Activity of Novel Fish Gelatin-Alginate Sponge (FGAS) Prototype

Heri Herliana ^{1*}, Harmas Yazid ², Avi Laviana ³, Ganesha Wandawa ⁴ and Basril Abbas ⁵

¹ Doctoral Program, Faculty of Dentistry, Universitas Padjadjaran, Bandung 45124, Indonesia

² Department of Oral and Maxillofacial Surgery, Faculty of Dentistry, Universitas Padjadjaran, Bandung 45124, Indonesia

³ Department of Orthodontics, Faculty of Dentistry, Universitas Padjadjaran, Bandung 45124, Indonesia

⁴ The Indonesian Naval Dental Institute, Jakarta 10210, Indonesia

⁵ Research Center for Radiation Process Technology, National Research and Innovation Agency (NRIA), Jakarta Indonesia

* Correspondence: heri21002@mail.unpad.ac.id; Tel.: +6281220153689)

Abstract: A hemostatic sponge prototype was successfully synthesized from fish gelatin as an alternative to mammalian gelatin, which was mixed with alginate in certain combinations and double cross-linking of calcium ions and gamma irradiation at a dose of 20 kGy to improve the characteristics and effectiveness of its function as a local hemostatic agent. There was an improvement in the physicochemical and mechanical properties, porosity index, absorption capacity, biodegradation properties, biocompatibility, and hemocompatibility of the FGAS prototypes compared with the pure fish gelatin sponge. Hemostatic activity tests showed that the means of clotting time, prothrombin time, and activated partial thromboplastin time were shorter in the FGAS prototype than in the negative control, and there was no significant difference compared with the commercial gelatin sponge. The hemostatic mechanism of the FGAS prototype combined a passive mechanism as a concentrator factor and an active mechanism through the release of calcium ions as a coagulation factor in the coagulation cascade process.

Keywords: fish gelatin; alginate; hemostatic sponge; blood coagulation

1.. Introduction

Uncontrolled bleeding is one of the leading causes of death in medical emergencies in civilian and military life. Approximately 80% of deaths in trauma cases in civilian society and 20% in the military are caused by exsanguination. Another cause is complications during surgical procedures, in which uncontrolled bleeding is the most common complication.[1,2] The risk of morbidity and mortality will increase in surgical procedures, especially in cases of uncontrolled bleeding, because it can be life-threatening.[3,4] Despite the proper use of conventional techniques for hemorrhage control to avoid such complications when uncontrolled bleeding occurs, a broad range of hemostatic agents are available as adjunctive measures to enhance hemostasis.[5] To treat excessive bleeding in areas that are difficult to access with conventional methods, a variety of topical hemostatic agents, including gelatin-based hemostatic agents, can be used and are currently available on the market.[6]

One of the most commonly used local hemostatic agents, especially after surgical procedures, is a mechanical hemostatic agent made from gelatin material in the shape of an absorbent sponge.[7] Gelatin is made from the denaturation of collagen-derived proteins through a limited thermohydrolysis process and is known as an essential natural biopolymer. It has the property to change shape reversibly between sol and gel.[8,9] The sources of gelatin as raw materials for biomaterials, including hemostatic sponges, are still dominated by mammalian gelatin from pigs and cows. Currently, the sources of gelatin used in the world originate from 46% pork skins, 29.4% cow skins, 23.1% beef bones, and 1.5% other sources such as poultry and fish.[7,9]

Using gelatin from mammals such as pigs and cows is restricted because of religious and infectious disease concerns. Both Muslim and Jewish communities are prohibited from consuming pork-based products, and Hindu communities reject bovine-based products. Both Muslim and Jewish communities are prohibited from consuming pork-based products, and Hindu communities reject bovine-based products. Furthermore, some animal-borne infectious diseases, such as bovine spongiform encephalopathy (BSE) in cows and swine flu in pigs, pose a threat to human health.[10,11] Therefore, another source of gelatin, for example, fish gelatin, has recently been required as an alternative to mammalian gelatin.

Fish gelatin has been widely researched and developed as an alternative source of mammalian (cow and pig) gelatin. However, fish gelatin has shortcomings in terms of physicochemical properties, mechanical strength, and gel stability compared with mammalian gelatin.[12] To improve the weak properties of fish gelatin, the mixing method can be used with other biopolymers, one of which is alginate, to form a gelatin-alginate composite compound. Alginate, which is found in many seaweeds, is also a natural polymer that is widely used in the biomedical field. One of the alginate salts, calcium alginate, is effective as a hemostatic agent. The fish gelatin-alginate composite can be further increased in its physicochemical properties using cross-linking methods, for example, by Ca^{2+} ionic cross-linking and gamma irradiation.[13,14]

This research aims to synthesize a prototype of a fish gelatin-alginate hemostatic sponge using blending methods, double cross-linking with calcium ions, and gamma irradiation, and then characterize and test the effectiveness of its hemostatic function in the blood coagulation process.

2. Materials and Methods

2.1. Materials

Gelatin (Redman fish gelatin, food grade 200 bloom, and viscosity of $3.45\text{mPa}\cdot\text{s}$) was purchased from Phoon Huat Pte. Ltd. (Singapore). Sodium alginate (analytical grade with a viscosity of $17\text{mPa}\cdot\text{s}$) and Calcium Chloride (CaCl_2) were purchased from Sigma-Aldrich Corporation (America), and commercial gelatin hemostatic sponges (Ceraspon) were purchased from PT Swayasa Perkasa (Indonesia). The other reagents used in this study were at least analytically pure.

2.2. Methods

2.2.1. Synthesis of The Fish Gelatin-Alginate Sponge (FGAS) Prototype

First, fish gelatin and sodium alginate powder were blended in a beaker containing double-distilled water to obtain a 4% (w/v) mixed solution with a certain proportion of fish gelatin (FG) and sodium alginate (SA) of 100/0, 75:25, 50:50, and 25:75. The solutions were then stirred evenly for 2 h at 50°C and then cast in a silicon mold to a size of $1\times 1\times 1\text{ cm}$, and frozen at -20°C . The frozen fish gelatin-alginate composites, except for the composition of 100:0 (pure fish gelatin), were then immersed in 2% CaCl_2 to provide ionic crosslinking between alginate and Ca^{2+} and produce a calcium alginate compound. In the next step, the Ca^{2+} crosslinked materials were then lyophilized with a freeze dryer at -50°C for 24 h to obtain the fish gelatin-alginate sponge (FGAS) prototype. The final procedure was gamma irradiation crosslinking of the prototype materials at a 20 kGy dose. The prototype was prepared at the Research Center for Radiation Process Technology, Jakarta. All procedures were performed according to previous studies, with some modifications.[15–22]

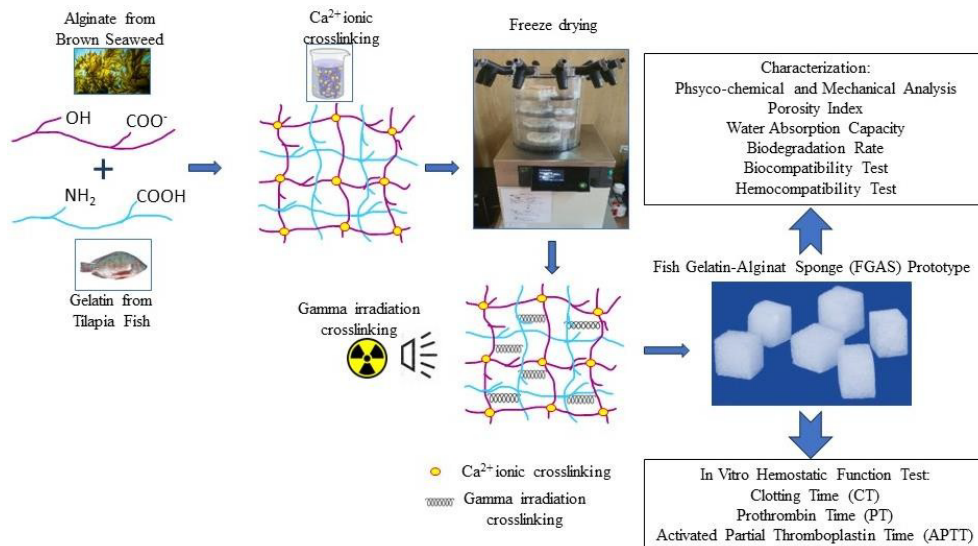


Figure 1. Diagrammatic representation of the research process.

2.2.2. Physicochemical and Mechanical Characterization

A scanning electron microscope (SEM) was used to analyze the surface morphology of the prototype, followed by chemical element analysis using the energy-dispersive X-ray spectroscopy (EDX/EDS) method. The samples were additionally coated with a metal (e.g., gold or platinum) before examination to avoid sample charging and increase contrast when imaging under high vacuum conditions. The analysis of the FGAS prototype functional groups was performed using Fourier transform infrared (FTIR) spectroscopy. All samples were prepared by grinding and mixing with KBr before being analyzed using an FTIR instrument. The mechanical properties were measured using the compressive strength test to determine the elasticity modulus of the FGAS prototype in wet conditions.[23–25]

2.2.3. Porosity Index Analysis

Porosity is an essential characteristic of sponge materials because it may directly impact the amount of water or blood they can absorb. There are various methods for measuring the porosity index of materials, including software like OriginPro and ImageJ.[26–28] We used OriginPro software to convert the images from SEM to quantitative measurements.

2.2.4. Water Absorption Capacity

The swelling test is a standard procedure for analyzing the absorption capacity of materials. The dry sponge (W_0) was weighed and placed in a pH 7.4 PBS solution for 30 min. The sponge gel was then wiped with filter paper to remove the residual solution from the sponge surface and weighed again (W_1). The sponge's water absorption rate was calculated using the following formula:[29]

$$\text{Water absorption rate (\%)} = (W_1 - W_0) / W_0 \times 100$$

2.2.5. Biodegradation Rate

The dry sponge (W_0) was weighed and placed in a pH 7.4 PBS solution at 37 °C for 1, 7, 14, and 30 days. On each day, the sponge was removed to dry, and then the sponge was weighed again (W_1). The weight retention (%) was calculated using the following equation:[30]

$$\text{Weight retention (\%)} = (W_0 - W_1) / W_0 \times 100$$

2.2.6. Biocompatibility (Cytotoxicity Test)

The cytotoxicity test was performed according to the ISO 10993-5 standard. The sponges produced were incubated on BHK-21 fibroblasts for 24, 48, and 72 h to measure cell viability by the MTT (3-(4,5- dimethylthiazol-2-yl)-2,5-diphenyltetrazolium bromide) assay. Cell viability was measured by reading the optical density (OD) of the sample, control, and blank with an Elisa reader and converting it to the following formula:[31]

$$\text{Cell viability (\%)} = \frac{\text{OD}_{\text{sample}} - \text{OD}_{\text{blank}}}{\text{OD}_{\text{control}} - \text{OD}_{\text{blank}}} \times 100$$

2.2.7. Hemocompatibility (Hemolysis Test)

Hemocompatibility is an essential criterion for any biomaterial that will interact closely with blood. The sponge samples were evaluated by hemolytic tests according to ISO 10993-4. Each of these samples was mixed with 0.4 mL of the incubated blood sample individually. Normal saline and deionized water were used as negative (neg) and positive (pos) controls, respectively. After completing all of the hemolysis assay steps, all samples were centrifuged at 3000 rpm for 5 min. Finally, the absorbance of the supernatants was determined at 545 nm using a UV-Vis spectrophotometer and counted using the following equation:[32]

$$\text{Hemolysis rate (\%)} = \frac{\text{OD}_{\text{sample}} - \text{OD}_{\text{neg control}}}{\text{OD}_{\text{pos control}} - \text{OD}_{\text{neg control}}} \times 100$$

2.2.8. Clotting Time (CT)

The in vitro clotting time was determined using the previously described method. Each sponge sample was placed in a clean test tube. The tubes were then immersed in a water bath at a constant temperature of 37°C for 1 h. Anticoagulated fresh donor blood (1 mL) was added to each of the test tubes and placed in the water bath. The tubes were tilted at 30° every 30 s until the blood in the tubes stopped flowing.[21] The coagulation times of blood in various tubes were recorded.

2.2.9. Prothrombin Time (PT)

Prothrombin time (PT) is the in vitro clotting time test after placing the PT reagent, which contains thromboplastin (phospholipids with tissue factor), calcium, and citrated plasma.[33] A platelet-poor plasma (PPP) sample was obtained by centrifuging fresh human blood at 3000 g for 10 min. Each sponge sample (1.0 cm³) received 500 µL of PPP and was incubated for 30 min at 37°C. To measure PT, combine 100 µL of PT reagent with 200 µL of PPP in a test tube and incubate at 37°C for 3 min. PT was then measured using an automated blood coagulation analyzer (COAX Bio System, Jerman). To serve as a control group, 500 µL of PPP extracted from fresh human blood was incubated at 37°C for 30 min without any test material.

2.2.10. Activated Partial Thromboplastin Time (APTT)

The APTT test measures the time it takes for plasma to clot in vitro after adding calcium, an activator of the intrinsic pathway, and the APTT reagent, which contains phospholipid, a platelet substitute that lacks tissue factor.[33] A platelet-poor plasma (PPP) sample was obtained by centrifuging fresh human blood at 3000 g for 10 min. Each sponge sample (1.0 cm³) received 500 µL of PPP and was incubated for 30 min at 37°C. To measure APTT, incubate 100 µL of PPP with 100 µL of reagent at 37°C for 3 min. Finally, 100 mL of aqueous calcium chloride (CaCl₂) was added to the solution, and the coagulation analyzer was used to determine the APTT value. To serve as a control group, 500 µL of PPP extracted from fresh human blood was incubated at 37°C for 30 min without any test material.

2.3. Statistical Analysis

The experimental results are presented as the mean ± SD. The data was analyzed using the one-way ANOVA method for studies with more than two treatment groups and the independent sample t-test method for studies with only two treatment groups.

3.. Results and Discussion

3.1. Synthesis of the Fish Gelatin-Alginate Sponge (FGAS) Prototype

This research produced a fish gelatin-alginate sponge prototype, which was synthesized by mixing and freeze-drying methods from fish gelatin and sodium alginate with Ca²⁺ ions and gamma irradiation cross-linking, and was proven to have hemostatic characteristics and effectiveness against blood clotting. The FGAS prototype is a white sponge, cube-shaped, and has an interconnected porous structure containing chemical elements and functional groups combined from gelatin and alginate, as well as additional calcium ions.

At a larger gelatin composition (75:25), the sponge prototype material appeared cuboid with flat and straight edges. The addition of alginate compositions (50:50 and 25:75) changed the shape of the sponge prototype to become more rounded at each corner. This is thought to be caused by an increase in the alginate composition, causing more cross-linking between alginate and Ca²⁺ ions to form an “egg-box model” structure. This structure is formed by an ionic bond between the Ca²⁺ ions and the carboxyl group on the guluronic block of the alginate polymer chain, thereby forming a stable bond in the alginate gelation process.[34,35] The formation of more egg-box model structures due to increasing alginate concentration can cause shrinkage and compaction of the sponge material, starting at the weakest corner points, so that the sponge containing more alginate becomes rounded at the corners.[36]

3.2. Physicochemical and Mechanical Characterization

The results of the SEM examination in Figure 2 show the surface morphology of the FGAS prototype, consisting of a porous structure with varying porous sizes with an average size between 39.03 – 266.66 µm. These porous sizes qualify as hemostatic sponges, as reported by previous research, which states that a porous size of between 50-100 µm is sufficient to accommodate the concentration of red blood cells and platelets in the initial process of blood clotting.[37] According to the IUPAC (International Union of Pure and Applied Chemistry) criteria, sponge material with a porous size of >50 µm is included in the macroporous category, which is ideal for containing cell concentrations because, in general, the average cell size is <100 µm.[38]

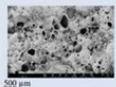
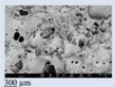
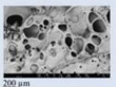

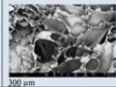
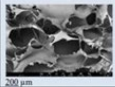

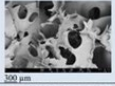

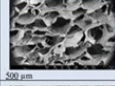

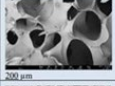
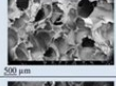
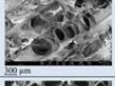
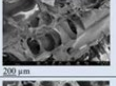


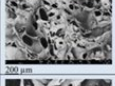
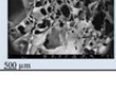
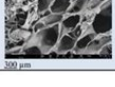
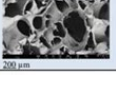
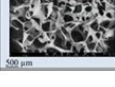

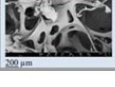
Samples	Magnification			Samples	Magnification		
	300 X	500 X	700 X		300 X	500 X	700 X
Pure Fish Gelatin (PFG)				FGAS _{75:25} Irradiated			
FGAS _{75:25} Non irradiated				FGAS _{50:50} Irradiated			
FGAS _{50:50} Non irradiated				FGAS _{25:75} Irradiated			
FGAS _{25:75} Non irradiated				Comercial Gelatin Sponge (CGS)			

Figure 2. SEM examination of the surface morphology of the FGAS prototype with magnifications of 300, 500, and 700X shows interconnected porous material.

The SEM images can also be used to analyze the chemical element content of the FGAS prototype combined with energy-dispersive X-ray spectroscopy (EDX/EDS) analysis, as shown in Table 1. The

main chemical element composition of the FGAS prototype material consists of carbon (C), nitrogen (N), oxygen (O), and calcium (Ca). The element content corresponds to the main elements contained in the raw materials, namely fish gelatin and alginate, which consist of C, N, O, and H. The H element cannot be detected using EDX analysis because it is very light. Calcium (Ca) is an additional element formed by cross-linking sodium alginate with Ca^{2+} ions in the CaCl_2 solution.[39]

Table 1. Chemical Elements Composition of The FGAS Prototype.

Sample	Composition	Chemical Elements (wt%)			
		Carbon (C)	Nitrogen (N)	Oxygen (O)	Calcium (Ca)
1	PFGS	22.478	21.578	16.583	-
2	FGAS _{75:25} Nir	5.506	12.613	10.711	30.030
3	FGAS _{50:50} Nir	6.300	4.600	9.800	25.600
4	FGAS _{25:75} Nir	1.800	1.900	5.300	18.700
5	FGAS _{75:25} Ir	20.500	27.000	8.900	22.000
6	FGAS _{50:50} Ir	18.418	15.516	14.715	19.119
7	FGAS _{25:75} Ir	17.700	6.900	16.700	17.700
8	CGS	35.200	33.900	30.900	-

PFGS: pure fish gelatin sponge, FGAS: fish gelatin-alginate sponge, Nir: non-irradiated, Ir: Irradiated, CGS: commercial gelatin sponge.

The analysis of the FGAS prototype functional groups was carried out using the Fourier transform infrared (FTIR) test to observe the wavelength spectrum in the form of specific peaks that indicate the functional groups possessed by the material, as shown in Figure 3 below.

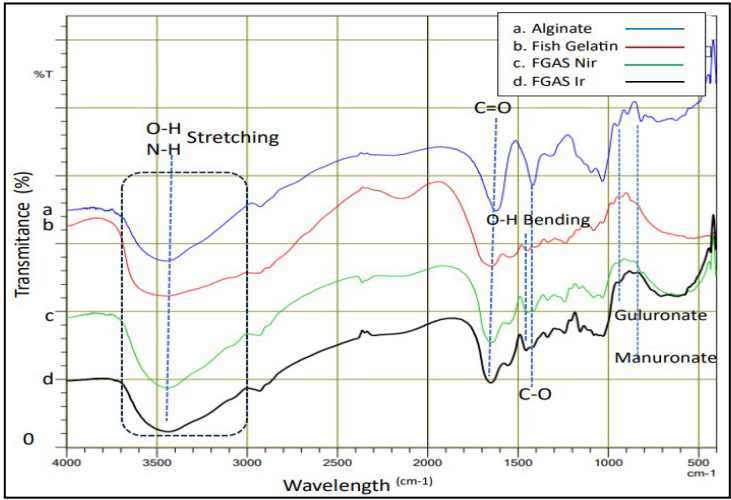


Figure 3. FTIR Spectra of Alginate, Gelatin, and The FGAS Prototypes.

Figure 3 shows the peaks of the infrared light absorption spectrum for typical functional groups found in gelatin polymers, alginate, and gelatin-alginate composites. Gelatin includes hydroxyl groups (O- H) and amine groups (N-H) at peak 3435.28cm^{-1} (superimposed) and carbonyl (C=O) at 1653.99cm^{-1} . Alginate includes hydroxyl (O-H) at 3439.14cm^{-1} ; carbonyl (C=O) at 1621.20cm^{-1} ; carboxyl (C-O) at 1314.51cm^{-1} ; guluronate and mannuronate fingerprints at 894.99cm^{-1} and 819.76cm^{-1} . The FTIR spectrum that appears in the gelatin-alginate composite is a combination of the spectrum of functional groups from gelatin and alginate polymers. The effect of gamma radiation can be seen from the shift in the absorption peaks of functional groups toward larger wavelengths in the group of samples that received gamma irradiation. these findings confirmed the previous studies of Sow et al., Derkach et al., and Hariyanti et al.[18,40,41]

The compressive strength test is a method for determining the mechanical properties of a biomaterial by measuring the elastic modulus, which is an important parameter in analyzing the

characteristics of a sponge-shaped biomaterial that will be applied as a local hemostatic agent.[42] Sponge elastic modulus measurement was performed in wet conditions according to the purpose of hemostatic sponge application in bleeding situations.

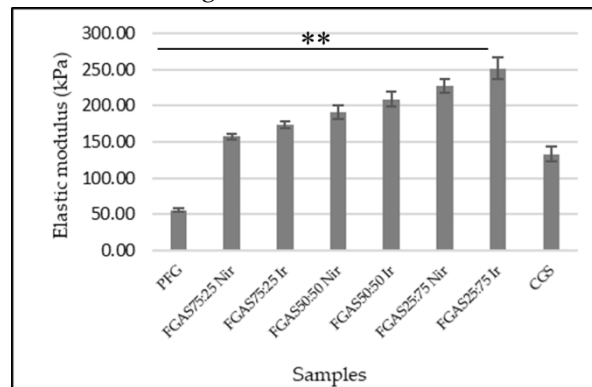


Figure 4. Modulus Elastic of The FGAS Prototypes in Wet Conditions (**p < 0.01).

All sponge samples show greater elasticity modulus mean compared with PFGS and were statistically significant. The FGAS_{75:25 Nir} and FGAS_{75:25 Ir} (157,79±3.99 and 173,86±5.18) have the closest values of elastic modulus to commercial gelatin sponges (133,54±9,79), but there was no significant difference in elastic modulus between irradiated and non-irradiated samples. Fish gelatin has low mechanical strength, especially in a single form, therefore, modifications are needed both in the synthesis method and by adding reinforcement materials to increase it.[43,44]

The increase in the elastic modulus of the FGAS prototype is thought to be due to the addition of alginate, resulting in an increase in density and shrinkage of the polymer chain caused by the formation of a model egg-box structure due to the ionic cross-linking reaction between the guluronate residue of the alginate polymer and the divalent cation Ca²⁺. As reported by Ma et al., in the preparation of fish gelatin hydrogel mixed with alginate, there was an increase in the elastic modulus.[45]

3.3. Porosity Index Analysis

Porosity is an essential characteristic of sponge materials because it may directly impact the amount of water or blood they can absorb, and these characteristics are strongly reliant on the underlying structure and morphology of sponges.[26,27] We analyzed the porosity index using OriginPro software, and the results are shown in Figure 5. All FGAS samples showed greater porosity index means compared with PFGS and were statistically significant.

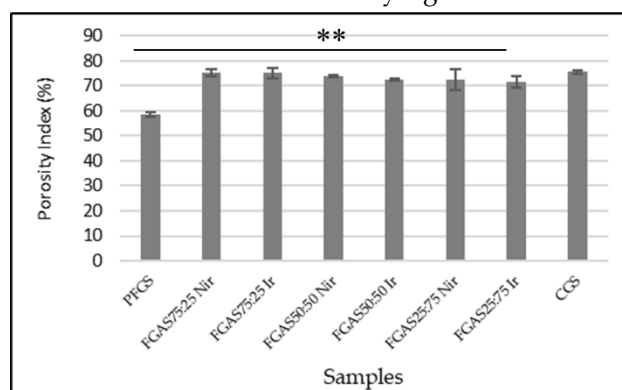


Figure 5. Porosity Index of FGAS Prototypes (**p < 0.01).

The addition of alginate increases the porosity index of the FGAS prototype above the standard value of 60% for all FGAS prototype compositions, both irradiated and non-irradiated, namely between 71.67% and 75.32%.46. The porosity indices of FGAS_{75:25 Nir} and FGAS_{75:25 Ir} have the largest means (75.33%±1.25 and 75.07%±2.15) compared to all samples and have no significant difference

compared to CGS. This is thought to be due to the addition of alginate, which is hydrophilic and binds water more strongly than fish gelatin during mixing so that when the lyophilization process (freeze-drying) is performed, it leaves more pores in the FGAS prototype material.[47] Sponge's highly porous nature makes it easier for them to absorb blood fluid, which in turn minimizes the amount of excess exudate. Similarly, the spongy hemostatic agents and wound dressings rely on the sponge's absorption properties which depend on the shape and structure of the sponges.[26–28] The comparison between irradiated and non-irradiated samples shows that there was no significant difference in the porosity index.

3.4. Water Absorption Capacity

Absorbing fluid or blood is one of the main requirements for materials with high absorption capacity, such as local hemostatic sponges.[29] The results of the water absorption rate of the FGAS prototype are shown in Figure 6, where all FGAS samples show greater water absorption rates than PFGS and are statistically significant.

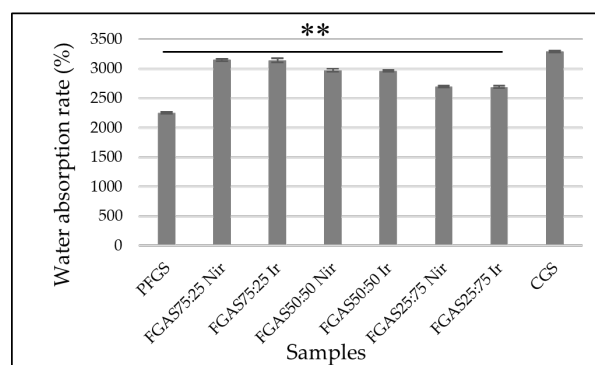


Figure 6. Water Absorption Capacity of FGAS Prototypes (** $p < 0.01$).

The addition of alginate can increase the absorption capacity ratio of the FGAS prototype. As seen in Figure 6, the FGAS_{75:25} Nir and FGAS_{75:25} Ir prototypes have the largest mean absorption capacity of 3147.45 ± 19.87 and 3141.58 ± 34.22 , respectively, and a significant difference statistically compared to the mean absorption capacity of PFGS. This is possible because of the addition of alginate, which has greater hydrophilic properties, so it can bind more water molecules. During the lyophilization process, the bound water molecules will be sublimated, leaving many spaces or pores in the material.[48] There was no significant difference in the water absorption capacity between the irradiated and non-irradiated samples.

3.5. Biodegradation Rate

The biodegradation rate of the FGAS prototype can be measured by counting the weight retention after immersing the sponge in a solution for a certain period.[30] The results of the biodegradation rate of the FGAS prototype are shown in Figure 7, where all sponge samples showed slower degradation rates compared with PFGS.

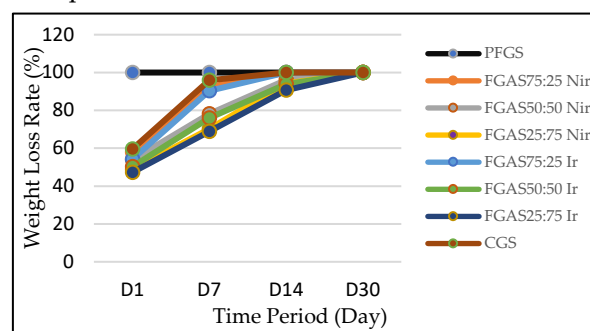


Figure 7. Biodegradation Rates of FGAS Prototypes.

On Day 1 of observation, the FGAS prototype group, both irradiated and non-irradiated, showed a smaller weight loss ratio compared with PFGS, which was completely dissolved (100%) and did not qualify as a hemostatic sponge. The rapid degradation of pure fish gelatin sponge (PFGS) is thought to be due to the amino acid hydroxyproline content in fish gelatin being lower than that of mammalian gelatin, causing a low solubility (melting point) at a temperature of 25 °C–27 °C compared with mammalian gelatin at 32 °C – 35 °C.[49] This was confirmed by Yang et al., who reported that pure gelatin sponges without cross-linking can immediately dissolve when immersed in PBS solution.[50]

The FGAS prototype has a slower biodegradation ratio than PGFS, allegedly due to the addition of alginate and the presence of ionic cross-linking with Ca²⁺ to form calcium alginate compounds, which are difficult to dissolve in water, plus the combination of hydrogen bonds between gelatin and alginate molecules, which are strengthened by covalent bonds through cross-linking by gamma irradiation.[30,51] On Days 7, 14, and 30, it was shown that FGAS_{75:25} Nir and FGAS_{75:25} Ir have similar weight loss rates to CGS. There was also a significant difference in biodegradation rates between irradiated and non-irradiated FGAS samples. This proves that gamma irradiation can strengthen the bonds between peptide molecules in gelatin and between functional groups of gelatin and alginate through covalent bonds.[52,53]

3.6. Biocompatibility (Cytotoxicity Test)

Based on the MTT Assay test results presented in Figure 8, it can be seen that all samples show an average viability of above 70% and no significant differences, which means that all samples meet the biocompatibility requirements according to the ISO 10993-5 standard.[54]

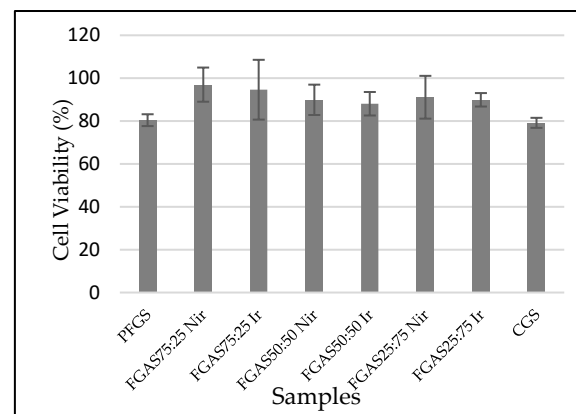


Figure 8. Cytotoxicity Test of FGAS Prototypes.

The cytotoxicity test results prove that all FGAS prototypes, both irradiated and non-irradiated have non-cytotoxic properties. Statistical testing using one-way ANOVA revealed no significant differences in the mean cell viability values for all research samples. These results confirmed several previously studies, such as Rezaie et al., who synthesized a highly absorbent sponge from bovine gelatin and sodium alginate by cross-linking using CaCl₂. The results of the cytotoxicity test on human fibroblast cells showed that the viability of all test samples was above 80%.[16] Another study reporting the effect of gamma irradiation at a dose of 25 kGy on the cytotoxicity of gelatin-alginate bioadhesive material showed that the average overall fibroblast cell viability value was in the range of 89–100%.[52]

3.7. Hemolysis Test

The hemolysis test results as presented in Figure 9 show that all samples show significant differences in erythrocyte hemolysis rates but are still below 5%, which means that all samples met the hemocompatibility requirements according to the ISO 10993-4 standard.[32]

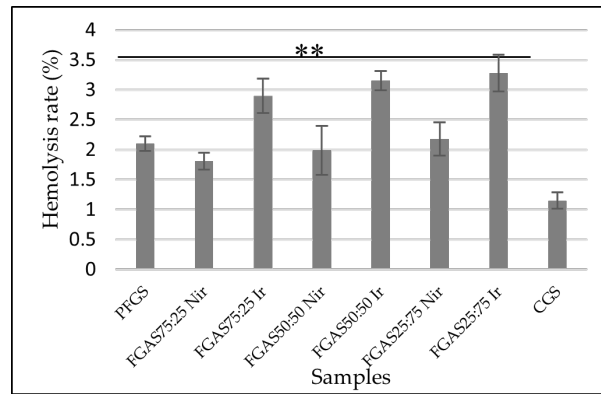


Figure 9. Hemocompatibility Rate of FGAS Prototypes (**p < 0.01).

There was also a significant difference in hemolysis rates between irradiated and nonirradiated FGAS samples. These findings confirmed the results of previous research by Rallapalli et al., who reported the effect of gamma irradiation at a dose of 25 kGy as a sterilization method on bovine pericardium scaffolds on the hemolysis ratio. There was an increase in the average hemolysis ratio from 1.8% before irradiation to 6.32% after irradiation. The increase in the hemolysis ratio is considered due to the irradiation process causing damage to the surface of the biomaterial, which becomes rougher so that it can damage erythrocytes and result in the lysis of hemoglobin.[55]

Hemocompatibility characteristics are an important requirement for assessing interactions between drugs or biomaterials that function or are related to the circulatory system. Hemocompatible drug compositions or materials are capable of interacting with blood components without causing clinically significant adverse reactions such as thrombosis, hemolysis, complement activation, or other adverse side effects.[56]

3.8. Hemostatic Activity Test

At this stage, the hemostatic function effectiveness test was only performed on the best FGAS prototype which resulted from the characterization test in the previous stage, where the FGAS_{75:25 Nir} and FGAS_{75:25 Ir} were found to be the selected prototypes.

3.8.1.. Clotting Time (CT)

Based on the results of the blood clotting time test, as shown in Figure 10, the mean clotting time for the FGAS_{75:25 Nir} prototype was 294.33±24.36 seconds and the FGAS_{75:25 Ir} prototype was 297.17±19 seconds, significantly different compared with the negative control (485.00±24.36 seconds), but not significantly different than CGS (272.33±22.47 seconds). There was no significant difference in clotting time between the irradiated and non-irradiated samples.

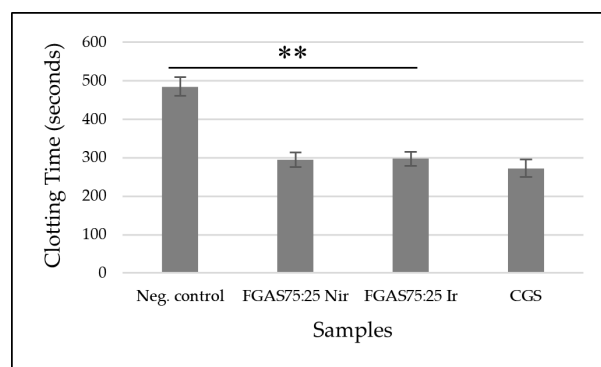


Figure 10. The Clotting Time of FGAS Prototypes (**p < 0.01).

The FGAS prototype has an effective function as a local hemostatic agent by accelerating the bleeding time due to the porous structure of the hemostatic sponge, which allows it to absorb a lot of blood fluid while concentrating coagulation components, red blood cells, and platelets. Immediately upon contact with blood, the hemostatic sponge causes adhesion and aggregation of platelets, which in turn causes the formation of a platelet plug, thereby preventing blood flow from the wound. It also triggers the release of blood clotting factors involved in the extrinsic and intrinsic coagulation pathways, resulting in formation of a stable blood clot that helps control bleeding from wounds.[37]

Several previous studies have confirmed the use of gelatin and alginate as local hemostatic agents, including research by Dai et al., who reported that the manufacture of gelatin (GA), calcium alginate (CA), and silk fibroin (SF) composite sponges had good effectiveness by speeding up bleeding time.[57] Chen et al. reported that the synthesis of gelatin-alginate hemostatic sponge with the addition of curcumin was effective in accelerating blood clotting time and preventing tumor recurrence.[30]

3.8.2. Prothrombin Time (PT)

Figure 11 shows that the FGAS_{75:25} Nir and FGAS_{75:25} Ir prototypes have the shortest mean prothrombin time, 10.9 ± 0.52 and 11.1 ± 0.59 seconds, respectively, and significant difference compared with the negative control (10.9 ± 0.52 seconds) but not significant difference than CGS (11.7 ± 0.48 seconds). There was also no significant difference in prothrombin time between the irradiated and non-irradiated samples.

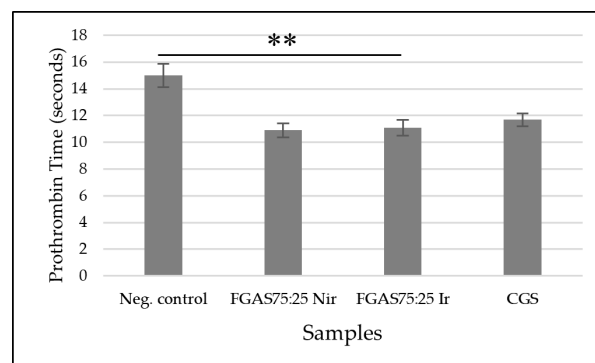


Figure 11. Prothrombin Time of FGAS Prototypes (**p < 0.01).

The effectiveness of the FGAS prototype in accelerating prothrombin time (PT) is considered due to the content of calcium ions bound in alginate. When in contact with blood, the FGAS prototype turns into a hydrogel, and a reaction occurs that encourages the entry of calcium ions into the wound through an ion exchange reaction with sodium ions in the blood. Furthermore, calcium ions trigger the production of coagulation factors VII, IX, and X, as well as platelets, activate the coagulation cascade reaction, and accelerate the hemostasis process.[58]

Previous research has reported the role of calcium alginate in the coagulation process because it contains phytohemagglutinin, which can trigger red blood cell aggregation and change erythrocyte morphology, exposing phosphatidylserine on the surface of erythrocytes and accelerating the conversion of local prothrombin to thrombin.[59] Dai et al. reported the hemostatic effectiveness of a composite sponge made from silk fibroin, gelatin, and calcium alginate by accelerating prothrombin time.[57]

3.8.3. Activated Partial Thromboplastin Time (APTT)

The results of the APTT test, as shown in Figure 12, show that the FGAS_{75:25} Nir and FGAS_{75:25} Ir prototypes have the shortest APPT means, namely 32.88 ± 0.78 and 33.18 ± 1.64 seconds, respectively, which is significantly different from the negative control (41.12 ± 0.63), but there is no significant difference with CGS (33.92 ± 0.63). There was also no significant difference in the APTT means between the irradiated and non-irradiated samples.

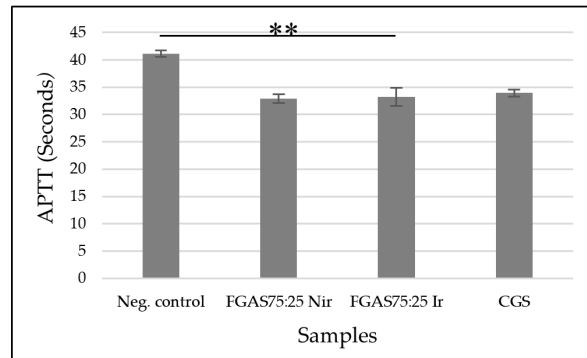


Figure 12. Activated Partial Thromboplastin Time of FGAS Prototypes (**p < 0.01).

Similar to the PT test, the APTT test results also suggested that the ability of the FGAS prototype to accelerate APTT was due to the calcium ion content bound in the alginate that was released when the sponge came into contact with the blood and then promoted the cascade coagulation process.[58]

As reported by Che et al. in making a polyelectrolyte multilayer film on a sodium alginate/gelatin sponge, it has the effectiveness of shortening APTT, which is thought to be due to the activity of the calcium ions contained in the sponge.[60] Another study by Kumar et al. stated that the synthesis of calcium alginate- zinc chloride hydrogel is determined by the content of calcium ions, which can trigger clotting factors in the coagulation cascade process.[61]

5.. Conclusions

The FGAS prototype has better physicochemical and mechanical characteristics, porosity index, water absorption capacity, biodegradation rate, biocompatibility, and hemocompatibility than PFGS where the FGAS_{75:25Nir} and FGAS_{75:25Ir} are selected as the best prototype composition. It is also proven that the FGAS prototype is effective as a local hemostatic agent, where the hemostatic mechanism is a combination of a passive mechanism as a concentrator factor through superiority in porosity index and absorption capacity, functioning as a matrix to collect blood cells, especially platelets, and coagulation factors, and the active mechanism through the content of calcium ions (Ca²⁺), which are released in the coagulation cascade process. The gamma irradiation of 20kGy dose only has an effect in the biodegradation and hemolysis rate characteristics of the FGAS prototype.

Author Contributions: Heri Herliana was responsible for conceptualization, formal analysis, and writing. Harmas Yazid was responsible for reviewing and supervising. Avi Laviana was responsible for editing and reviewing. Ganesha Wandawa was responsible for editing and directing. Basril Abbas was responsible for the methodology, resources, and field supervision.

Funding: This study received no external funding.

Institutional Review Board Statement: The study was conducted in accordance with the Declaration of Helsinki and approved by the Ethics Committee of Indonesian Marine Hospital (Number: 18/X/2023/RSMC, date of approval: 30th October 2023).

Data Availability: This article includes all data presented or analyzed during the study.

Acknowledgments: We thank the Doctoral Program Faculty of Dentistry, Universitas Padjadjaran, and the National Research and Innovation Agency (NRIA), for their technical support.

Conflicts of Interest: The authors declare that they have no conflicts of interest or personal relationships that could have influenced the work presented in this paper.

References

1. Gordy SD, Rhee P, Schreiber MA. Military applications of novel hemostatic devices. *Expert Rev Med Devices*. 2011;8(1):41–7.

2. Malik A, Rehman FU, Shah KU, Naz SS, Qaisar S. Hemostatic strategies for uncontrolled bleeding: A comprehensive update. *J Biomed Mater Res - Part B Appl Biomater*. 2021;109(10):1465–77.
3. Nagarale R, Todkar M, Khan S, Khan Y, Rehan M, Rizvi Q. Assessment of knowledge, importance and management of uncontrolled bleeding in dental surgical procedures among dental professionals. *Int J Appl Dent Sci*. 2021;7(4):312–6.
4. de Campos N, Furlaneto F, Buischi YDP. Bleeding in dental surgery. In: *Contemporary Applications of Biologic Hemostatic Agents across Surgical Specialties-Volume 2*. IntechOpen; 2019.
5. Chiara O, Cimbanassi S, Bellanova G, Chiarugi M, Mingoli A, Olivero G, et al. A systematic review on the use of topical hemostats in trauma and emergency surgery. *BMC Surg*. 2018;18(1):1–20.
6. Irfan NI, Mohd Zubir AZ, Suwandi A, Haris MS, Jaswir I, Lestari W. Gelatin-based hemostatic agents for medical and dental application at a glance: A narrative literature review. *Saudi Dent J [Internet]*. 2022; Available from: <https://doi.org/10.1016/j.sdentj.2022.11.007>.
7. Herliana H, Yusuf HY, Laviana A, Wandawa G, Cahyanto A. Characterization and Analysis of Chitosan-Gelatin Composite-Based Biomaterial Effectivity as Local Hemostatic Agent: A Systematic Review. *Polymers (Basel)*. 2023;15(3):575.
8. Rather JA, Akhter N, Ashraf QS, Mir SA, Makroo HA, Majid D, et al. A comprehensive review on gelatin: Understanding impact of the sources, extraction methods, and modifications on potential packaging applications. *Food Packag Shelf Life [Internet]*. 2022; 34 (September):100945. Available from: <https://doi.org/10.1016/j.fpsl.2022.100945>.
9. Alipal J, Mohd Pu'ad NAS, Lee TC, Nayan NHM, Sahari N, Basri H, et al. A review of gelatin: Properties, sources, process, applications, and commercialisation. *Mater Today Proc [Internet]*. 2019;42:240–50. Available from: <https://doi.org/10.1016/j.matpr.2020.12.922>.
10. Nurilmala M, Suryamarevita H, Husein Hizbullah H, Jacoeb AM, Ochiai Y. Fish skin as a biomaterial for halal collagen and gelatin. *Saudi J Biol Sci [Internet]*. 2022;29(2):1100–10. Available from: <https://doi.org/10.1016/j.sjbs.2021.09.056>.
11. Ahmed MA, Al-Kahtani HA, Jaswir I, AbuTarboush H, Ismail EA. Extraction and characterization of gelatin from camel skin (potential halal gelatin) and production of gelatin nanoparticles. *Saudi J Biol Sci [Internet]*. 2020;27(6):1596–601. Available from: <https://doi.org/10.1016/j.sjbs.2020.03.022>.
12. Huang T, Tu Z, Shanguan X, Sha X, Wang H, Zhang L, et al. Fish gelatin modifications: A comprehensive review. *Trends Food Sci & Technol*. 2019;86:260–9.
13. Rajeswari A, Stobel Christy EJ, Pius A. Biopolymer blends and composites [Internet]. *Biopolymers and their Industrial Applications*. Elsevier Inc.; 2021. 105–147 p. Available from: <http://dx.doi.org/10.1016/B978-0-12-819240-5.00005-5>.
14. Toh HW, Toong DWY, Ng JCK, Ow V, Lu S, Tan LP, et al. Polymer blends and polymer composites for cardiovascular implants. *Eur Polym J [Internet]*. 2021;146(January):110249. Available from: <https://doi.org/10.1016/j.eurpolymj.2020.110249>.
15. Lou CW, Huang MS, Chang CY, Lu CT, Chen WC, Lin JH. Preliminary study in cross-linked gelatin/alginate sponges. *Appl Mech Mater*. 2012;184–185:1102–5.
16. Rezaie A, Mehdipour A, Salmanipour S, Alipour N, Salehi R. Highly Porous Alginate/Gelatin Sponge For Hemostasis Of Severe Femoral Bleeding In Rats. *Stud Med Sci [Internet]*. 2023;33(12). Available from: <http://umj.umsu.ac.ir/article-1-5968-en.html>.
17. Song Y, Xu L, Xu L, Deng L. Radiation cross-linked gelatin/sodium alginate/carboxymethylcellulose sodium hydrogel for the application as debridement glue paste. *Polym Bull [Internet]*. 2022;79(2):725–42. Available from: <https://doi.org/10.1007/s00289-020-03525-5>.
18. Hariyanti, Erizal, Apriyani RZ, Perkasa DP, Lestari I, Rahmi H. Synthesis of Polyvinyl Alcohol (PVA)-Gelatin Hydrogel from White Snapper (*Lates calcarifer*, Bloch) with Gamma Irradiation and Its Characterizations. *Atom Indones*. 2023;49(2):69–75.
19. Lu H, Butler JA, Britten NS, Venkatraman PD, Rahatekar SS. Natural antimicrobial nano composite fibres manufactured from a combination of alginate and oregano essential oil. *Nanomaterials*. 2021;11(8):1–17.
20. Haug IJ, Draget KI, Smidsrød O. Physical and rheological properties of fish gelatin compared to mammalian gelatin. *Food Hydrocoll*. 2004;18(2):203–13.
21. Hu Z, Ouyang QQ, Cheng Y, Hong PZ, Liao MN, Chen FJ, et al. Optimization of preparation process and characterization of carboxymethyl chitosan/sodium alginate hemostatic sponge. *IOP Conf Ser Mater Sci Eng*. 2017;213(1).
22. Kang HJ, Jo C, Lee NY, Kwon JH, Byun MW. A combination of gamma irradiation and CaCl₂ immersion for a pectin-based biodegradable film. *Carbohydr Polym*. 2005;60(4):547–51.
23. Kuo ZK, Lai PL, Toh EKW, Weng CH, Tseng HW, Chang PZ, et al. Osteogenic differentiation of preosteoblasts on a hemostatic gelatin sponge. *Sci Rep [Internet]*. 2016;6(September):1–12. Available from: <http://dx.doi.org/10.1038/srep32884>.

24. Koch M, Włodarczyk-Biegun MK. Faithful scanning electron microscopic (SEM) visualization of 3D printed alginate-based scaffolds. *Bioprinting* [Internet]. 2020;20:e00098. Available from: <https://doi.org/10.1016/j.bprint.2020.e00098>.
25. Dai F, Zhuang Q, Huang G, Deng H, Zhang X. Infrared Spectrum Characteristics and Quantification of OH Groups in Coal. *ACS Omega*. 2023;8(19):17064–76.
26. Li G, Quan K, Liang Y, Li T, Yuan Q, Tao L, et al. Graphene-Montmorillonite Composite Sponge for Safe and Effective Hemostasis. *ACS Appl Mater Interfaces*. 2016;8(51):35071–80.
27. Hojat N, Gentile P, Ferreira AM, Siller L. Automatic pore size measurements from scanning electron microscopy images of porous scaffolds. *J Porous Mater* [Internet]. 2023;30(1):93–101. Available from: <https://doi.org/10.1007/s10934-022-01309-y>.
28. Tasya AY, Kusumawati DH. Karakteristik Porositas Wound Dressing Nanofiber PVA-Ekstrak Daun Nangka. *J Inov Fis Indonesia* [Internet]. 2023;12:106–12. Available from: <https://ejournal.unesa.ac.id/index.php/inovasi-fisika-Indonesia/>.
29. Wang QQ, Liu Y, Zhang CJ, Zhang C, Zhu P. Alginate/gelatin blended hydrogel fibers cross-linked by Ca²⁺ and oxidized starch: Preparation and properties. *Mater Sci Eng C* [Internet]. 2019;99(February):1469–76. Available from: <https://doi.org/10.1016/j.msec.2019.02.091>.
30. Chen K, Pan H, Yan Z, Li Y, Ji D, Yun K, et al. A novel alginate/gelatin sponge combined with curcumin-loaded electrospun fibers for postoperative rapid hemostasis and prevention of tumor recurrence. *Int J Biol Macromol* [Internet]. 2021;182:1339–50. Available from: <https://doi.org/10.1016/j.ijbiomac.2021.05.074>.
31. Sharifi S, Maleki Dizaj S, Ahmadian E, Karimpour A, Maleki A, Memar MY, et al. A Biodegradable Flexible Micro/Nano-Structured Porous Hemostatic Dental Sponge. *Nanomaterials*. 2022;12(19).
32. Sahadat Hossain M, Shaikh MAA, Jahan SA, Mahmud M, Bin Mobarak M, Rahaman MS, et al. Exploring the biomedical competency of gamma-radiation aided hydroxyapatite and its composite fabricated with nano-cellulose and chitosan. *RSC Adv*. 2023;13(14):9654–64.
33. Chee YL. Coagulation. *J R Coll Physicians Edinb*. 2014;44(1):42–5.
34. Pulat M, Ozukaya D. Preparation and Characterization of Na-Alginate Hydrogel Beads. 2019;6:32–8. Available from: www.isres.org.
35. Kaur N, Singh B, Sharma S. Hydrogels for potential food application: Effect of sodium alginate and calcium chloride on physical and morphological properties. ~ 142 ~ *Pharma Innov J* [Internet]. 2018;7(7):142–8. Available from: www.thepharmajournal.com.
36. Zhang X, Wang K, Hu J, Zhang Y, Dai Y, Xia F. Role of a high calcium ion content in extending the properties of alginate dual-crosslinked hydrogels. *J Mater Chem A*. 2020;8(47):25390–401.
37. Nepal A, Tran HDN, Nguyen NT, Ta HT. Advances in haemostatic sponges: Characteristics and the underlying mechanisms for rapid haemostasis. *Bioact Mater*. 2023;27:231–56.
38. Ebrahimi M. Porosity parameters in biomaterial science: Definition, impact, and challenges in tissue engineering. Vol. 15, *Frontiers of Materials Science*. 2021. 352–373 p.
39. Taheraslani M, Gardeniers H. High-Resolution SEM and EDX Characterization of Deposits Formed by CH₄ + Ar DBD Plasma Processing in a Packed Bed Reactor. 2019.
40. Sow LC, Toh NZY, Wong CW, Yang H. Combination of sodium alginate with tilapia fish gelatin for improved texture properties and nanostructure modification. *Food Hydrocoll* [Internet]. 2019;94:459–67. Available from: <https://doi.org/10.1016/j.foodhyd.2019.03.041>.
41. Derkach SR, Voron'ko NG, Sokolan NI, Kolotova DS, Kuchina YA. Interactions between gelatin and sodium alginate: UV and FTIR studies. *J Dispers Sci Technol* [Internet]. 2020;41(5):690–8. Available from: <https://doi.org/10.1080/01932691.2019.1611437>.
42. Yang G, Huang Z, McCarthy A, Huang Y, Pan J, Chen S, et al. Super-Elastic Carbonized Mushroom Aerogel for Management of Uncontrolled Hemorrhage. *Adv Sci*. 2023;10(16):1–17.
43. Xing Q, Yates K, Vogt C, Qian Z, Frost MC, Zhao F. Increasing mechanical strength of gelatin hydrogels by divalent metal ion removal. *Sci Rep*. 2014;4:1–10.
44. Atma Y. Synthesis and application of fish gelatin for hydrogels/ composite hydrogels: A review. *Biointerface Res Appl Chem*. 2022;12(3):3966–76.
45. Ma C, Choi JB, Jang YS, Kim SY, Bae TS, Kim YK, et al. Mammalian and fish gelatin methacryloyl- alginate interpenetrating polymer network hydrogels for tissue engineering. *ACS Omega*. 2021;6(27):17433–41.
46. Cuicui D, Kuan C, Yue W, Yifan Y, Xiaohong C, Jingyi L, et al. Dual green hemostatic sponges constructed by collagen fibers disintegrated from *Halocynthia roretzi* by a shortcut method. *Mater Today Bio*. 2024;24:1–12.
47. Afjoul H, Shamloo A, Kamali A. Freeze-gelled alginate/gelatin scaffolds for wound healing applications: An in vitro, in vivo study. *Mater Sci Eng C* [Internet]. 2020;113:110957. Available from: <https://doi.org/10.1016/j.msec.2020.110957>.
48. Saarai A, Kasparkova V, Sedlacek T, Saha P. A comparative study of crosslinked sodium alginate/gelatin hydrogels for wound dressing. *Recent Res Geogr Geol Energy, Environ Biomed - Proc 4th WSEAS Int Conf EMESEG'11, 2nd Int Conf WORLD-GEO'11, 5th Int Conf EDEB'11*. 2011;384–9.

49. Al-Nimry S, Dayah AA, Hasan I, Daghmash R. Cosmetic, Biomedical and Pharmaceutical Applications of Fish Gelatin/Hydrolysates. *Mar Drugs*. 2021;19(3).
50. Yang G, Xiao Z, Long H, Ma K, Zhang J, Ren X, et al. Assessment of the characteristics and biocompatibility of gelatin sponge scaffolds prepared by various crosslinking methods. *Sci Rep [Internet]*. 2018;8(1):1–13. Available from: <http://dx.doi.org/10.1038/s41598-018-20006-y>.
51. Junkyu S. Evaluation of Calcium Alginate Microparticles Prepared Using a Novel Nebulized Aerosol Mediated Interfacial Crosslinking Method. University of Toledo; 2016.
52. Foox M, Ben-Tzur M, Koifman N, Zilberman M. Effect of gamma radiation on novel gelatin alginate- based bioadhesives. *Int J Polym Mater Polym Biomater*. 2016;65(12):611–8.
53. Syed M, Azam N, Moni N, Gobetti A, Ramorino G. Advances in Modulating Mechanical Properties of Gelatin-Based Hydrogel in Tissue Engineering. 2023.
54. Gruber S, Nickel A. Toxic or not toxic? The specifications of the standard ISO 10993-5 are not explicit enough to yield comparable results in the cytotoxicity assessment of an identical medical device. *Front Med Technol*. 2023;5(June):1–14.
55. Rallapalli S, Liman AM, Guhathakurta S. Hemocompatibility and surface properties of bovine pericardial patches: Effects of gamma sterilization. *Curr Med Res Pract [Internet]*. 2016;6(6):224–8. Available from: <http://dx.doi.org/10.1016/j.cmrp.2016.10.001>.
56. Nalezinková M. In vitro hemocompatibility testing of medical devices. *Thromb Res [Internet]*. 2020;195(July):146–50. Available from: <https://doi.org/10.1016/j.thromres.2020.07.027>.
57. Dai M, Li M, Gong J, Meng L, Zhang B, Zhang Y, et al. Silk fibroin/gelatin/calcium alginate composite materials: Preparation, pore characteristics, comprehensive hemostasis in vitro. *Mater Des [Internet]*. 2022;216(199):110577. Available from: <https://doi.org/10.1016/j.matdes.2022.110577>.
58. Xie Y, Gao P, He F, Zhang C. Application of Alginate-Based Hydrogels in Hemostasis. *Gels*. 2022;8(2).
59. Wang L, Li W, Qin S. Three polymers from the sea: Unique structures, directional modifications, and medical applications. *Polymers (Basel)*. 2021;13(15).
60. Che C, Liu L, Wang X, Zhang X, Luan S, Yin J, et al. Surface-Adaptive and On-Demand Antibacterial Sponge for Synergistic Rapid Hemostasis and Wound Disinfection. *ACS Biomater Sci Eng*. 2020;6(3):1776–86.
61. Kumar A, Sah DK, Khanna K, Rai Y, Yadav AK, Ansari MS, et al. A calcium and zinc composite alginate hydrogel for pre-hospital hemostasis and wound care. *Carbohydr Polym [Internet]*. 2023;299(September 2022):120186. Available from: <https://doi.org/10.1016/j.carbpol.2022.120186>.

Disclaimer/Publisher's Note: The statements, opinions and data contained in all publications are solely those of the individual author(s) and contributor(s) and not of MDPI and/or the editor(s). MDPI and/or the editor(s) disclaim responsibility for any injury to people or property resulting from any ideas, methods, instructions or products referred to in the content.